ELSEVIER

Catalysis Today 84 (2003) 173–180

CATALYSIS TODAY

www.elsevier.com/locate/cattod

Effects of pH and surface modification of TiO_2 with SiO_x on the photocatalytic degradation of a pyrimidine derivative

Han-Su Lee [a], Tak Hur [a], Shawn Kim [b], Jae-Hyun Kim [a], Ho-In Lee [a,*]

[a] *School of Chemical Engineering and Research Center for Energy Conversion and Storage, Seoul National University, San 56-1, Sillim-dong, Gwanak-gu, Seoul 151-744, South Korea*

[b] *BATU Enviro-Tek Inc., San 48-1, Gongheung-ri, Yangpyeong-eup, Yangpyeong-gun, Gyounggi-do 476-800, South Korea*

Abstract

A pyrimidine derivative, 2-isopropyl-6-methyl-4-pyrimidinol (IMP), could be completely decomposed following pseudo-first-order kinetics by photocatalytic reaction using TiO_2. The effects of pH and surface modification of TiO_2 with SiO_x were studied. The degradation rate of IMP was fast in mild acidic condition (pH = 6.3) and slower in strong acidic (pH = 2.0) or basic (pH = 10.0) condition. The main reason of the slow IMP degradation was different in strong acidic and basic conditions. In strong acidic condition, the slow degradation rate was explained by electrostatic repulsion. On the other hand, a little formation of hydroxyl radicals was considered as a main reason in strong basic condition. The result was supported by the experiments using SiO_x-loaded TiO_2, which has a lower isoelectric point than pure TiO_2.

Keywords: pH; SiO_x; Pyrimidine derivative; Electrostatic repulsion; Isoelectric point

1. Introduction

Recently, heterogeneous photocatalysis is attracting worldwide interests for water treatment. TiO_2 is mainly used as a catalyst for heterogeneous photocatalysis due to its high photocatalytic activity and physicochemical stability [1–3]. There are many factors to affect photocatalysis: for example, the physical property of TiO_2 according to synthesis procedure [4–6], property of reactant [7], pH condition during photocatalysis [8–10], and so on. Heterogeneous photocatalysis consists of two important steps: the first step is the generation of active species (hole, electron, and hydroxyl radical) by light excitation and the second step is the contact of active species with reactant by adsorption of reactant on the catalyst surface or diffusion of active species to the reactant. The latter may be mainly related to the surface property of the catalyst, the property of reactant, pH condition, and salt concentration in solution [11].

Pyrimidine compounds are found largely in biomolecules and agrochemicals. There have been several works about photocatalytic degradation of pyrimidine compounds [12–15]. They focused on the degradation mechanism of DNA bases (uracil, thymine, and cytosine) and ionic effects. These works are much attractive for water treatment and cancer treatment.

In this paper, we selected 2-isopropyl-6-methyl-4-pyrimidinol (IMP) as a pyrimidine derivative and studied the effect of pH on the photocatalytic degradation rate. In addition, we modified the surface of TiO_2 with SiO_x and surveyed the effect of surface modification of TiO_2.

* Corresponding author. Tel.: +82-2-880-7072; fax: +82-2-888-1604.
E-mail address: hilee@snu.ac.kr (H.-I. Lee).

0920-5861/$ – see front matter © 2003 Elsevier B.V. All rights reserved.
doi:10.1016/S0920-5861(03)00271-2

2. Experimental

2.1. Reagents and preparation of the catalysts

IMP was purchased from Aldrich and used as purchased. The photocatalyst TiO_2 was Degussa P-25 (particle size, 20–30 nm; crystal structure, 80% anatase and 20% rutile; surface area, 50 $m^2\,g^{-1}$). Two kinds of surface modified TiO_2 were prepared as follows. One was prepared by sol–gel method. Tetraethylorthosilicate (98%, Lancaster) was mixed with dehydrated ethanol (99.5%, Daejung). TiO_2 was added into the mixture. After sonication of the mixture, 1 M HCl was added into the mixture to progress sol–gel process. The mixture was stirred at room temperature for 24 h and the solvent was removed under vacuum condition at 40 °C for 6 h. The remaining powder was ground and calcined at 300 °C for 30 min. The other was prepared by impregnation method. Na_2SiO_3 (Chemical Pure grade, Junsei) was dissolved in deionized water. TiO_2 was added into the solution. After sonication, the mixture was stirred at 60–70 °C for 4 h. The mixture was dried at 110 °C for 48 h. The resultant paste was ground and calcined at 300 °C for 30 min.

2.2. Irradiation experiments

The static photoreactor was a Pyrex cylinder whose middle part was jointed with another Pyrex cylinder as a lamp window to cut off deep UV light of wavelength shorter than 300 nm. The operating temperature was controlled at 23 ± 1 °C by circulating cooling water through a large beaker in which the reaction vessel was immersed. The cooling water was also passed through the Pyrex cylinder in order to remove IR radiation. UV irradiation was carried out with a high-pressure mercury lamp (700 W, Kum-Kang). In each experiment, the concentration of catalyst was maintained with 200 mg l^{-1} and the total volume of solution was adjusted to 300 ml. The initial concentration of IMP was fixed at 80 mg l^{-1}. The initial pH of reaction solution was adjusted by adding 35% HCl and 1 M NaOH solution. After sonication of the mixture for 3 min, all the irradiation experiments were performed.

2.3. Analytical methods

The concentration and absorption coefficient (ε) of IMP in the filtered suspension were measured by a UV-Vis spectrophotometer (UV-2401PC, Shimadzu). The pH of the solution was measured by a proton ion selective electrode (Model 8102BN, Orion). The chemical oxygen demand (COD) of solution was determined by closed reflux and colorimetric method using dichromate ion as an oxidant [16]. Reaction products were analyzed by a GC–mass spectrophotometer (HP 6890 PLUS Gas Chromatograph and HP 5973 Mass Selective Detector, Hewlett Packard).

To get isoelectric points of the catalysts, zeta potential measurements of the catalysts were carried out with a zeta potential analyzer (Delsa 440SX, Coulter). BET surface area and pore size distribution were determined by N_2 adsorption using an ASAP 2010 apparatus at −196 °C. The samples were pretreated at 150 °C under high vacuum for 2 h. Pore size distribution was obtained from desorption isotherm by BJH method. The powder X-ray diffraction (XRD) was carried out on a Mac Science M18XHF22-SRA diffraction spectrometer using Cu Kα as a radiation source.

3. Results and discussion

3.1. Photocatalytic degradation

IMP was degraded only under both UV irradiation and TiO_2 presence conditions (Fig. 1). IMP was not

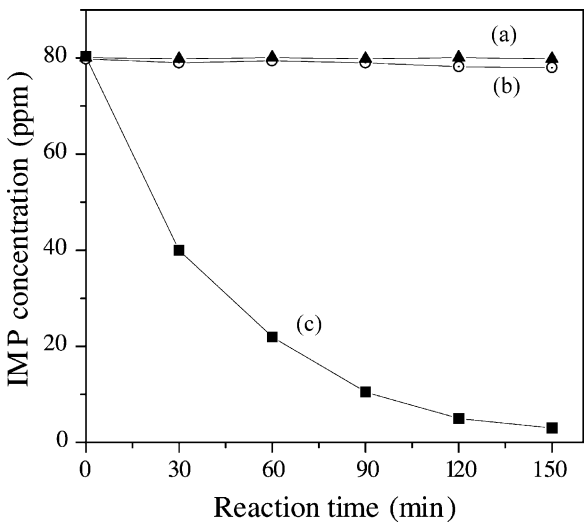

Fig. 1. Change of IMP concentration as a function of reaction time with: (a) only TiO_2; (b) only UV irradiation; (c) both TiO_2 and UV irradiation.

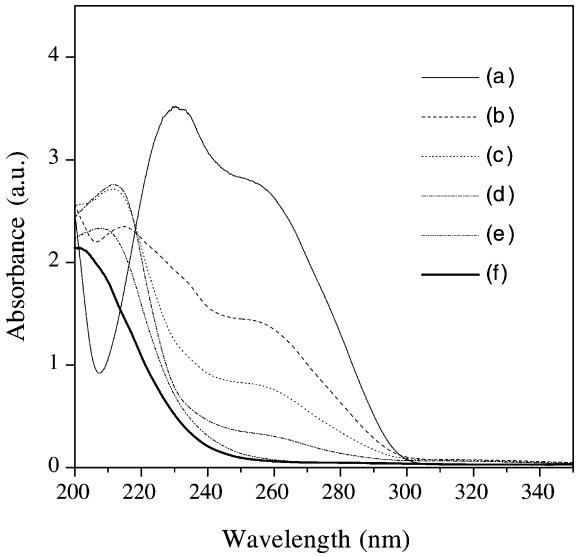

Fig. 2. Change of UV absorption spectrum of IMP after irradiation time of: (a) 0 min; (b) 30 min; (c) 60 min; (d) 90 min; (e) 4 h; (f) 8 h.

removed by adsorption on TiO_2 and very small amount of IMP was decomposed by direct photolysis. Fig. 1 shows that photocatalytic degradation of IMP follows a pseudo-first-order kinetics. In aqueous solution, the photocatalytic decomposition with suspended TiO_2 powder is known to follow Langmuir–Hinshelwood mechanism [17]. In dilute concentration of substrate, the reaction rate approximates to a first-order kinetics and is simply described by $-\mathrm{d}[c]/\mathrm{d}t = k[c]$, where $[c]$ is the concentration of the organic compound to be decomposed, and k the overall degradation rate constant [18]. The k contains both the reaction rate constant and the equilibrium adsorption coefficient. In this paper, the performance of photocatalysis was presented by overall degradation rate constant, k.

UV absorption spectrum changes of IMP with irradiation time are shown in Fig. 2. It demonstrates that IMP has two absorption peaks, which result from pyrimidine ring [19]. The first peak around 230 nm is from $\pi \rightarrow \pi^*$ transition and the second peak around 260 nm is from $n \rightarrow \pi^*$ one. Two peaks disappeared as the reaction progressed suggesting that pyrimidine ring opening took place by photocatalytic reaction. Acetamide, which might be a fragment of IMP ring, was also detected in the GC–mass analysis of reaction intermediates and the result supported again that pyrimidine ring opening progressed through photocatalysis. Fig. 3 shows the change of total organic material amount as a function of irradiation time. After most of the IMP molecules were decomposed, large amount of organic materials still remained. The remained organic materials were mineralized constantly with irradiation time. The above results suggest strongly that the overall degradation of IMP progresses via pyrimidine ring opening and then total mineralization of intermediates formed during reaction.

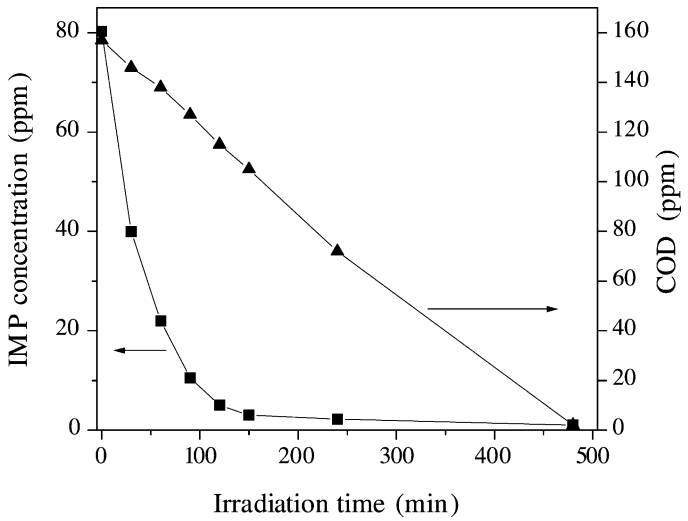

Fig. 3. Changes of IMP concentration and COD value as a function of irradiation time.

Table 1
Overall degradation rate constants and final pH values at different initial pH conditions

	Initial pH				
	2.0	4.0	6.3	7.5	10.0
Overall reaction rate constant, k (min^{-1})	0.0127	0.0201	0.0223	0.0194	0.0073
Coefficient of determination, R^2	0.9885	0.9776	0.9979	0.9908	0.9915
pH value after irradiation for 150 min	2.0	4.6	5.5	5.9	6.8

Horikoshi and Hidaka [15] also reported that ring opening took place in case of photocatalytic degradation of some nitrogen-containing heteroaromatics.

3.2. pH effect on the photocatalytic degradation rate

The influence of pH on the photocatalytic degradation rate was studied at various initial pH conditions. In acidic (pH = 4.0), mild acidic (pH = 6.3), and mild basic (pH = 7.5) conditions, the overall degradation rate constants were higher than those in strong acidic (pH = 2.0) and basic (pH = 10.0) conditions (Table 1 and Fig. 4). The highest overall degradation rate constant appeared at 6.3 of pH. The overall degradation rate decreased with the decrement or increment of pH from 6.3. This phenomenon could be explained by using charge state model.

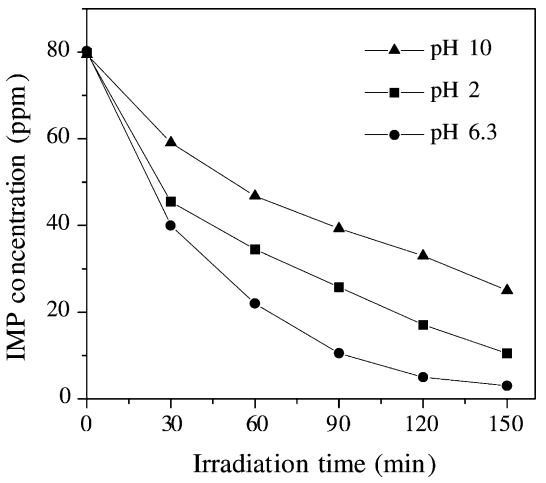

Fig. 4. Change of IMP concentration as a function of irradiation time at different pH's.

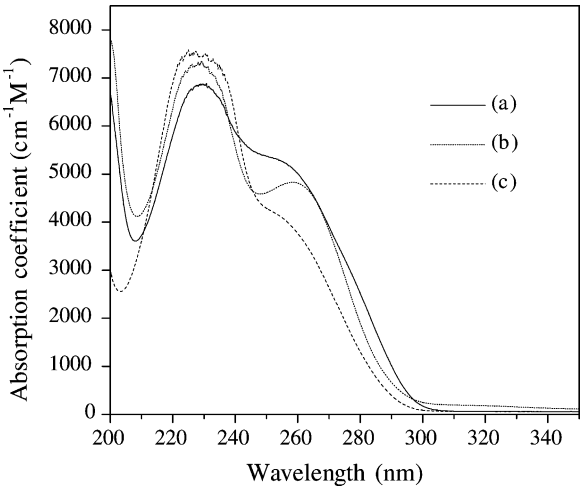

Fig. 5. Change of UV absorption coefficient of IMP at different pH's: (a) 6.3; (b) 10.0; (c) 2.0.

The UV absorption coefficient of IMP varied with pH (Fig. 5). Especially, that of n $\rightarrow$ π^* transition at about 260 nm lowered in strong acidic condition. The n $\rightarrow$ π^* transition is caused by non-bonding electrons of nitrogen in IMP. In strong acidic condition, non-bonding electrons can easily accept protons and IMP becomes protonated. As a result, the UV absorption coefficient of n $\rightarrow$ π^* transition lowered in strong acidic condition suggesting that positively charged IMP species exist in strong acidic condition. On the other hand, the dissociation of proton from the hydroxyl group of IMP easily happens in strong basic condition. The deprotonated IMP molecules exist as negatively charged species. Similar trend is also observed in other pyrimidine compounds. Some kinds of pyrimidinol compounds have two kinds of pK_a value. Acidic pK_a is about 6.78–9.17 and basic pK_a is about 1.87–2.24 [19]. Accordingly, IMP comes to be positive or negative depending on pH condition.

The surface charge state of TiO_2 also depends on pH condition. The isoelectric point of TiO_2 (P-25) was located at about 6.5 of pH (Table 2). The surface charge of TiO_2 becomes negative at pH above the isoelectric point and positive at pH below the isoelectric point. Accordingly, the surface hydroxyl of TiO_2 exists as

Table 2
Physical properties and isoelectric points of TiO_2 and SiO_x-loaded TiO_2's

Catalyst	Crystal structure	BET surface area ($m^2\,g^{-1}$)	Isoelectric point (pH)
TiO_2 (P-25)	Anatase 80%, rutile 20%	50	~6.5
0.5 mol% SiO_x-loaded TiO_2 (from sol–gel method)	Same as TiO_2	49	~5.5
0.5 mol% SiO_x-loaded TiO_2 (from impregnation method)	Same as TiO_2	48	~4.5

forms of $TiOH_2^+$ and TiO^- in strong acidic and basic conditions, respectively.

In consequence, both IMP and TiO_2 have the same kind of charge in strong acidic or basic condition resulting in electrostatic repulsion between IMP and TiO_2 (Scheme 1). As a result, active species like hydroxyl radical have such small possibilities of contacts with IMP that the overall degradation rate becomes lower. Nedoloujko and Kiwi [7] studied on the photocatalytic degradation of 4-*tert*-butylpyridine (*t*-BP). They showed that *t*-BP was so easily protonated below 5.99 of pH that it became positive similar to pyrimidine compounds and concluded that *t*-BP could not be decomposed by photocatalysis using TiO_2 because of the electrostatic repulsion between *t*-BP and TiO_2.

When the overall degradation rate constant in strong basic condition was compared with one in strong acidic condition, the overall degradation rate constant was lower in strong basic condition (Table 1). This implies that the effects of other factors exist besides electrostatic repulsion in strong basic condition. The mechanism for photocatalytic reaction by TiO_2 is shown below [9,20]:

$$TiO_2 \xrightarrow{h\nu} h^+ + e^- \quad (1)$$

$$H_2O + h^+ \rightarrow {}^\bullet OH + H^+ \quad (2)$$

$$OH_{(s)}{}^- + h^+ \rightarrow {}^\bullet OH \quad (3)$$

$$O_2 + e^- \rightarrow {}^\bullet O_2{}^- \quad (4)$$

$${}^\bullet O_2{}^- + H^+ \leftrightarrow {}^\bullet HO_2 \quad (pK_a = 4.88) \quad (5)$$

$${}^\bullet HO_2 + {}^\bullet HO_2 \rightarrow H_2O_2 + O_2 \quad (6)$$

$${}^\bullet O_2{}^- + {}^\bullet HO_2 \rightarrow HO_2{}^- + O_2 \quad (7)$$

$$HO_2{}^- + H^+ \rightarrow H_2O_2 \quad (8)$$

$$H_2O_2 + {}^\bullet O_2{}^- \rightarrow {}^\bullet OH + OH^- + O_2 \quad (9)$$

$$H_2O_2 \xrightarrow{h\nu} 2{}^\bullet OH \quad (10)$$

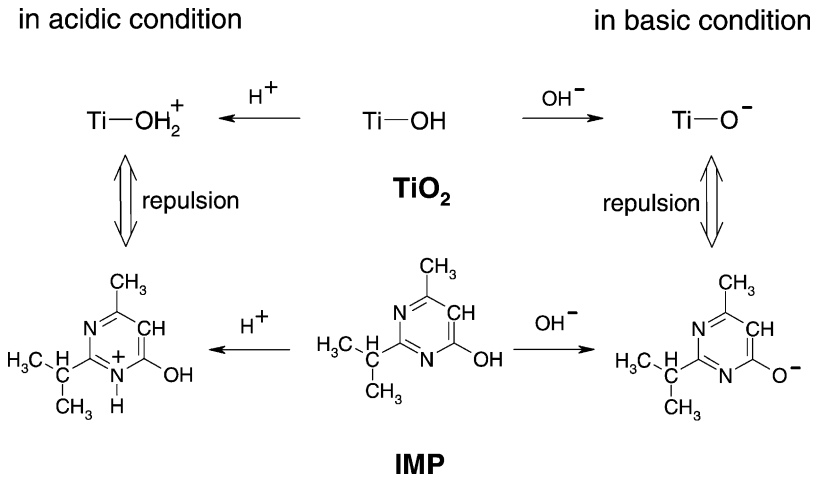

Scheme 1. Charge state changes of TiO_2 and IMP with pH condition.

In the higher pH region than pK_a (=4.88) for HO_2 radical, the reverse reaction of reaction (5) dominates and the reactions (6)–(10) do not proceed. As a result, the formation of OH radicals decreased in strong basic condition. If the reactions (6)–(10) do not proceed, OH^- does not form resulting in the decrease of pH value. Practically, pH value got down in strong basic condition as the reaction proceeded (Table 1). This result agreed with the above proposed mechanism.

Conduction and valence band edges increase at the rate −60 mV per unit increase of pH in strong basic condition [21]. This indicates that the oxidation ability of TiO_2 decreases in strong basic condition resulting in the decrease of the formation of OH radicals by hole.

Consequently, it is assumed that smaller formation of OH radicals caused overall degradation rate to be decreased in strong basic condition.

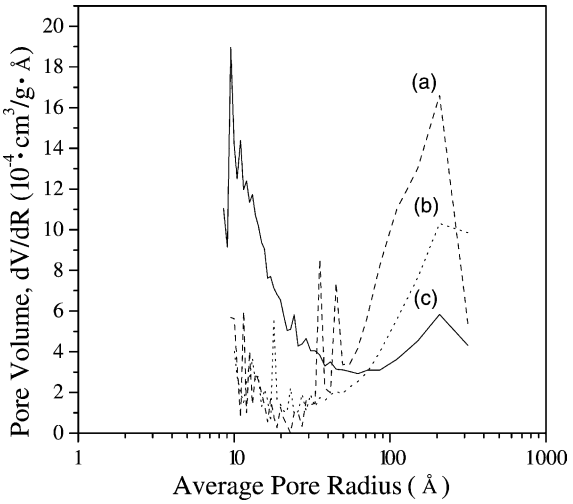

Fig. 6. Pore size distributions of catalysts: (a) 0.5 mol% SiO_x-loaded TiO_2 (from impregnation method); (b) 0.5 mol% SiO_x-loaded TiO_2 (from sol–gel method); (c) pure TiO_2.

3.3. Effect of surface modification with SiO_x

Two kinds of SiO_x-loaded TiO_2 were prepared by sol–gel method and conventional impregnation method. The physical properties of the prepared catalysts were compared with pure TiO_2 in Table 2 and Fig. 6. After SiO_x loading, the crystal structure did not change and the BET surface area decreased slightly. However, the isoelectric point and the pore size distribution were remarkably changed. The SiO_x loading on TiO_2 caused the increase of macropore and the drop of pH value of isoelectric point. Furthermore, the pore size distribution and the isoelectric point were different according to the method of SiO_x loading. Fig. 6 shows that macropore around 200 Å increased with SiO_x loading. Generally, the increase of macropore is considered as the result of particle agglomeration suggesting that the SiO_x loading caused the TiO_2 particle agglomeration and that the TiO_2 particle agglomeration took place much more in impregnation procedure. The TiO_2 particle agglomeration was thought to affect the overall degradation rate. Table 3 shows that the more agglomerated TiO_2 particle, the lower overall degradation rate constant at pH 6.3, where no effect of electrostatic repulsion existed. The TiO_2 particle agglomeration might cause the loss of active sites for photocatalysis.

Particularly, the changes of isoelectric points by SiO_x loading were more interesting. The isoelectric point of SiO_2 is known to be located at about pH 2. Table 2 shows that the isoelectric points of the catalysts were lowered after the loading of SiO_x on TiO_2. Because SiO_x is dispersed on the surface of TiO_2, the

Table 3
Overall degradation rate constants of TiO_2 and SiO_x-loaded TiO_2's at different initial pH conditions

Catalyst	Initial pH					
	2		6.3		10	
	k (min^{-1})	R^2	k (min^{-1})	R^2	k (min^{-1})	R^2
TiO_2 (P-25)	0.0127	0.9885	0.0223	0.9979	0.0073	0.9915
0.5 mol% SiO_x-loaded TiO_2 (from sol–gel method)	0.0180	0.9898	0.0206	0.9906	0.0079	0.9901
0.5 mol% SiO_x-loaded TiO_2 (from impregnation method)	0.0196	0.9976	0.0185	0.9980	0.0079	0.9956

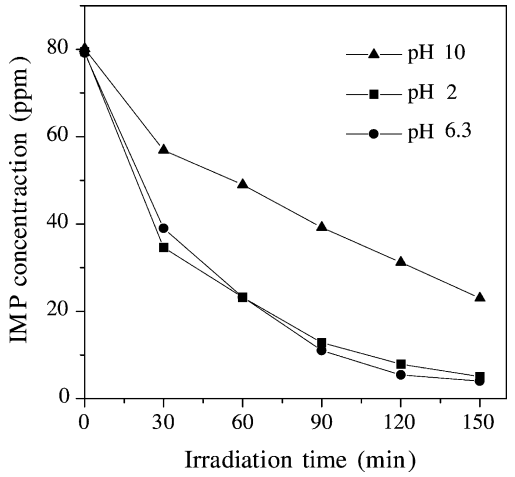

Fig. 7. Change of IMP concentration using 0.5 mol% SiO_x-loaded TiO_2 (from sol–gel method) at different pH's.

surface property of the catalyst would follow one of the SiO_x. These SiO_x-loaded TiO_2's showed higher activities than pure TiO_2 in strong acidic condition (Table 3 and Figs. 7 and 8). The result agrees with the preceding discussion about pH effect (3.2). SiO_x-loaded TiO_2 had lower isoelectric point. That implies that SiO_x-loaded TiO_2 has less positive surface charge than pure TiO_2 in strong acid condition. As the result, less electrostatic repulsion existed between the catalyst and IMP molecule in strong acidic condition resulting in easy reaction of active species like hydroxyl radical with IMP molecules under strong acidic condition. Consequently, the charge states of catalyst and IMP, giving electrostatic repulsion, were a very important factor on photocatalytic degradation of IMP in strong acidic condition.

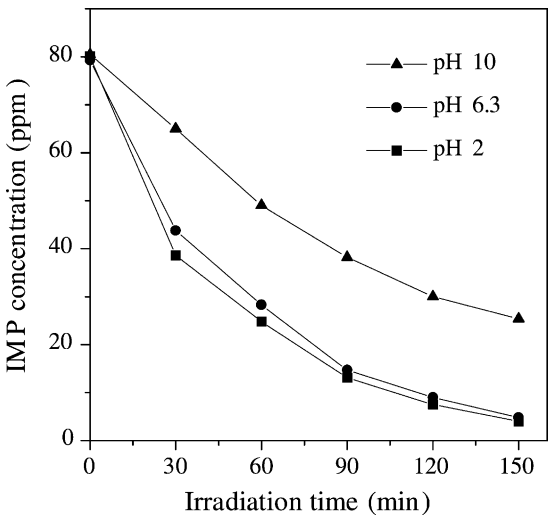

Fig. 8. Change of IMP concentration using 0.5 mol% SiO_x-loaded TiO_2 (from impregnation method) at different pH's.

However, strong basic condition gave a different situation. Because SiO_x-loaded TiO_2 had lower isoelectric point than pure TiO_2, the surface of SiO_x-loaded TiO_2 would be more negative than pure TiO_2 in strong basic condition. Being viewed in the electrostatic repulsion, there would be more electrostatic repulsion between SiO_x-loaded TiO_2 and IMP, and overall degradation rate should have been slower. Nevertheless, overall degradation rate constants were similar in the strong basic condition regardless of isoelectric points of the catalysts (Table 3). This suggests that the effect of electrostatic repulsion was not critical and the smaller formation of OH radicals was the main reason of slow reaction rate in strong basic condition.

The dependency of photocatalytic activity on the surface charge of the catalysts was also made sure when NaCl was added into the solution in the mild acidic condition. The effect of salt addition into the solution is very important. Especially, chloride is a well-known inhibitor in photocatalysis. When the concentration of NaCl was less than 500 mg l^{-1}, the reaction rate decreased slightly. This indicates that the small amount of Na^+ or Cl^- added for pH adjustment was not lethal to the photocatalytic oxidation of IMP. However, when the concentration of NaCl was 1500 mg l^{-1}, the reaction rate was dropped by 35 and 12% in the cases of pure TiO_2 and SiO_x-loaded TiO_2, respectively. In the mild acidic condition (pH 6.3), the surface charge of TiO_2 is slightly positive leading to electrostatic attraction between the catalyst and the chloride. On the contrary, SiO_x-loaded TiO_2 has a negatively charged surface to which chloride experiences difficulty getting access.

Besides the isoelectric point of TiO_2, SiO_x loading changed the surface hydration state of TiO_2. FT-IR analysis showed the surface hydroxyl group of TiO_2 decreased after SiO_x loading. However, we found that the surface hydroxyl group, related to hydrophilic–hydrophobic property, had no relationship to the reaction rate in this study.

4. Conclusions

IMP, a kind of pyrimidine derivative, could be decomposed by photocatalytic reaction using TiO_2. IMP was completely oxidized via ring opening reaction as the UV irradiation progressed. Photocatalytic degradation of IMP followed pseudo-first-order kinetics and the reaction rate was affected by pH condition. When using pure TiO_2 (P-25), of which isoelectric point was about 6.5 of pH, the degradation rate was the fastest in mild acidic condition (pH = 6.3). In strong acidic condition (pH = 2), both TiO_2 and IMP had same positive surface charges and the resultant electrostatic repulsion resulted in the slow degradation rate. In strong basic condition (pH = 10), the degradation rate also became slow. However, the main reason for the slow reaction rate in strong basic condition was considered not to be the electrostatic repulsion but the smaller formation of OH radicals at high pH values due to OH radical formation mechanism. By the loading of SiO_x on TiO_2, the agglomeration of TiO_2 particles took place resulting in the decrease of degradation rate in mild acidic condition due to the loss of active sites. However, SiO_x-loaded TiO_2 had lower isoelectric point than pure TiO_2, and as the result, the degradation rate over SiO_x-loaded TiO_2 was faster than that over pure TiO_2 in strong acidic condition because of less electrostatic repulsion in that condition. In strong basic condition, the SiO_x loading on TiO_2, which changed the isoelectric point of TiO_2, did not affect the degradation rate suggesting that the small formation of OH radicals was the main reason for the slow degradation rate.

Acknowledgements

This work was financially supported by the National Institute of Environmental Research through the Korea Institute of Environmental Science and Technology, and by the Korea Science and Engineering Foundation through the Research Center for Energy Conversion and Storage at Seoul National University.

References

[1] N. Serpone, R.F. Khairutdinov, Stud. Surf. Sci. Catal. 103 (1997) 417.
[2] C. Anderson, A.J. Bard, J. Phys. Chem. 99 (1995) 9882.
[3] K.S. Jung, H.-I. Lee, J. Korean Chem. Soc. 41 (1997) 682.
[4] J.F. Porter, Y.-G. Li, C.K. Chan, J. Mater. Sci. 34 (1999) 1523.
[5] Z. Ding, Q. Lu, P.F. Greenfield, J. Phys. Chem. B 104 (2000) 4815.
[6] K.Y. Jung, S.B. Park, Korean J. Chem. Eng. 18 (2001) 879.
[7] A. Nedoloujko, J. Kiwi, Water Res. 34 (2000) 3277.
[8] A. Houas, H. Lachheb, M. Ksibi, E. Elaloui, C. Guillard, J.-M. Herrmann, Appl. Catal. B 31 (2001) 145.
[9] K.-H. Wang, Y.-H. Hsieh, M.-Y. Chou, C.-Y. Chang, Appl. Catal. B 21 (1999) 1.
[10] H.-H. Chung, J.-S. Rho, J. Ind. Eng. Chem. 5 (1999) 81.
[11] M.M. Halmann, Photodegradation of Water Pollutants, CRC Press, Boca Raton, FL, 1996, Chapter 1, p. 1.
[12] M.R. Dhananjeyan, R. Annapoorani, S. Lakshmi, R. Renganathan, J. Photochem. Photobiol. A 96 (1996) 187.
[13] M.R. Dhananjeyan, R. Annapoorani, R. Renganathan, J. Photochem. Photobiol. A 109 (1997) 147.
[14] M.R. Dhananjeyan, V. Kandavelu, R. Renganathan, J. Mol. Catal. A 158 (2000) 577.
[15] S. Horikoshi, H. Hidaka, J. Photochem. Photobiol. A 141 (2001) 201.
[16] A.D. Eaton, L.S. Clesceri, A.E. Greenberg, Standard Methods for the Examination of Water and Wastewater, American Public Health Association, Washington, 1995, pp. 5–12.
[17] S.-S. Hong, C.-S. Ju, C.-G. Lim, B.-H. Ahn, K.-T. Lim, G.-D. Lee, J. Ind. Eng. Chem. 7 (2001) 94.
[18] Y.T. Kwon, K.Y. Song, W.I. Lee, G.J. Choi, Y.R. Do, J. Catal. 191 (2000) 192.
[19] D.J. Brown, S.F. Mason, The Pyrimidine, Wiley, New York, 1962, Chapter 13, p. 464.
[20] T. Hirakawa, Y. Nokada, Langmuir 18 (2002) 3247.
[21] N. Takeda, N. Iwata, T. Torimoto, H. Yoneyama, J. Catal. 177 (1998) 240.